Journal of Theoretical Biology 545 (2022) 111149

Contents lists available at ScienceDirect

Journal of Theoretical Biology

journal homepage: www.elsevier.com/locate/yjtbi

A quantitative method to project the probability of the end of an epidemic: Application to the COVID-19 outbreak in Wuhan, 2020

Baoyin Yuan [a], Rui Liu [a,b,*], Sanyi Tang [c,*]

[a] School of Mathematics, South China University of Technology, Guangzhou 510640, China
[b] Pazhou Lab, Guangzhou 510330, China
[c] School of Mathematics and Statistics, Shaanxi Normal University, Xi'an 710119, China

ARTICLE INFO

Article history:
Received 21 December 2021
Revised 21 April 2022
Accepted 25 April 2022
Available online 30 April 2022

Keywords:
Epidemic
End-of-outbreak
Nonpharmaceutical interventions
Effectiveness
Mathematical model

ABSTRACT

The end-of-outbreak declaration is an important part of epidemic control, marking the relaxation or cancellation of prevention and control measures. We propose a probability model to retrospectively quantify the confidence of giving the end-of-outbreak declaration during the COVID-19 epidemic in early 2020 in Wuhan. By using the linear spline, we firstly estimates the time-varying proportion of cases who miss the nonpharmaceutical interventions (NPIs) among all reported cases. Assuming the reproduction numbers being 1.5, 2.0, 3.0, 4.0, 5.0 and 6.0, the respective probability of the end of the COVID-19 outbreak with time after the last reported case can be iteratively computed. Consequently, the varying reproduction numbers produce slightly different increasing patterns of NPI effectiveness, and the end-of-outbreak declarations with 95% confidence are projected consistently earlier than the day when the lockdown was actually lifted. The reason for the timing discrepancy is discussed as well.

1. Introduction

Every pandemic of infectious diseases in history has posed a great threat to human life and health. In the current coronavirus disease 2019 (COVID-19) era, the disease has spread all over the world since it was first recognized in Wuhan, China, in early 2020, even though the natural source of the pathogen is still scientifically unknown. The ongoing COVID-19 pandemic is the most severe public health crisis since the 1918 influenza pandemic (Liang et al., 2021) and had caused more than 242 million infections and 4.92 million deaths throughout the world by October 22, 2021. The prevention and control of the epidemic has undergone nonpharmaceutical interventions (NPIs) (Kucharski et al., 2020), such as contact tracing, quarantine and isolation and social distancing from the beginning to the current vaccination stage (Rubin, 2021). Specific combinations of interventions have been implemented to control the spread of COVID-19 despite the differences in political and social backgrounds between countries. Basically, two different strategies can be generalized: 'zero COVID', adopted by China, Singapore, South Korea, Australia and New Zealand, and 'living with COVID', adopted by most of the other countries (Normile, 2021).

Since the beginning of the epidemic, China has adhered to the zero-case policy by carrying out strict entry quarantine and repeated nucleic acid tests and even enforcing the lockdown of an entire high-risk city. Multiple rounds of molecular testing for residents in the enclosed area provides the most direct evidence for understanding the real-time situation of the epidemic. In the past local outbreaks (Guangzhou Municipal Health Commission, 2021; The Health Commission of Hainan Province, 2021; Nanjing Municipal Health Commission, 2021) in China, such a strict policy has indeed achieved remarkable success in clearing infections. It is worth noting that there are three basic conditions for cancelling the epidemic restrictions, including no newly confirmed cases during the past 14 days, the full negative nucleic acid testing results of the residents and their living environments for at least three rounds, and all close contacts being effectively controlled, even though there are no universal standards applying to all the local outbreaks. These three epidemiological conditions currently used have proven to be relatively reliable in defining the end of the epidemic. The early or premature declaration of the end of an outbreak would put the population at risk of a resurgence of infections, while too late or delayed end-of-outbreak declaration would greatly increase the economic and social cost owing to repeated extensive molecular testing and the stagnation of social activity (Du et al., 2021; Atkeson et al., 2020; The British Academy, 2021; Elliott, 2020). Quantifying the end-of-outbreak confidence in the late stage of the epidemic on the basis of

* Corresponding authors at: School of Mathematics, South China University of Technology, Guangzhou 510640, China (R. Liu).
E-mail addresses: scliurui@scut.edu.cn (R. Liu), sytang@snnu.edu.cn (S. Tang).

https://doi.org/10.1016/j.jtbi.2022.111149
0022-5193/

mathematical models is of great significance to complement the current surveillance-based standards.

Djaafara et al. summarized the end-of-outbreak criteria for various pathogens in some past epidemics (Djaafara et al., 2021). Twice the longest length of the incubation period after the last confirmed case is most frequently recommended by the World Health Organization (WHO) to define the end of an epidemic, such as the MERS outbreak in South Korea in 2015, the Lassa Fever Outbreak in Benin in 2016 and the Ebola outbreak in the Democratic Republic of Congo in 2017. The other measure is employed based on the continuous monitoring of no new cases in the later stage of an epidemic, such as no new cases reported for six months in the 2015–2017 yellow fever outbreak in Angola and the Democratic Republic of the Congo (WHO, 2017) and no new cases reported for seven weeks in the 2017 cholera outbreak in South Sudan (WHO, 2018). When it comes to COVID-19, the upper bounds of the incubation period, *i.e.*, 14 days, are currently recommended for quarantine length by the CDC (Centers for Disease Control and Prevention, 2021). According to UKHSA (UK Health Security Agency, 2020), if there are no new test-confirmed cases for the shortest consecutive 28 days, the end of COVID-19 outbreak can be declared. Given that some of the surveillance-based criteria ignored the specific transmission dynamics under intervention and tended to make no immediate adjustments with the development of the epidemic, some more flexible mathematical models have been proposed to adapt to the specific epidemiological focus. Depending on the decision-maker's 'acceptable risk', the days with no cases to declare the outbreak was over would be substantially influenced by the surveillance sensitivity (Thompson et al., 2019). Parag et al. (2020) developed a probabilistic model based on the renewal process of infection propagation and thus quantified the probability of elimination at the tail of one generic disease outbreak. Moreover, the influence of the case reporting defects and migration between regions on the confidence of the end-of-outbreak declaration has been discussed. With the iteratively computed effective reproduction number by the method adapted from information theory, Parag and colleagues (Parag et al., 2021) design a model framework to quantify the confidence in epidemic elimination, where the local cases and imported cases are classified. A different simulation-based model was proposed in (Djaafara et al., 2021) by phasing the outbreak and projecting the incidence trajectory in the end-of-outbreak declaration phase. The authors concluded that the instantaneous reproduction number, the reporting rate and the illness onset day of the last case were the sensitive factors in declaring the end of the outbreak. One probabilistic model established by Nishiura (2016) and its modified versions involving reporting delay of the epidemic curve, defining the end of an epidemic via the cumulative distribution function of serial interval, were applied in the epidemics of MERS in South Korea, 2015 (Nishiura et al., 2016), Ebola in Africa in 2015–2016 (Lee and Nishiura, 2019), and the ongoing COVID-19 in Japan (Linton et al., 2021), in Taiwan Island (Akhmetzhanov et al., 2021). As we have emphasized, these methods only approached some specific epidemiological issues; for example, the authors of (Linton et al., 2021, Akhmetzhanov et al., 2021) especially concentrated on reporting delay and underreporting problems in the case reporting procedure when developing their end-of-outbreak model.

Different from the above models, our new modeling framework is developed to retrospectively quantify the end-of-outbreak confidence of the COVID-19 outbreak in early 2020 in Wuhan by accounting for the proportion of infective cases not covered by intervention restrictions. Now that this outbreak has been terminated, the actual ending declaration of the epidemic can help verify the predictive ability of the model. After the COVID-19 outbreak in Wuhan was recognized, various control measures were implemented, and the lockdown of the city started on January 23, 2020, strictly restricting the movement of people between cities. Within the city, extensive nonpharmaceutical interventions were carried out, dichotomizing all the infected cases into two types: type I cases, which were effectively isolated prior to developing infectiousness, and type II cases, which had a chance of further transmission due to imperfect interventions and which dominated the transmission mode of this outbreak. Thus, all secondary infections can be regarded as being caused by type II cases. Quantitative assessment of the ratio of the two types of cases is of critical significance for accurately understanding the transmission dynamics because it directly reflected the NPI effectiveness in cutting off the virus transmission between infected and susceptible people. Different mathematical forms as a function of time have been designed to describe the time-varying intervention effectiveness. For example, Tang et al. (2020) assumed an exponentially increasing quarantine rate of susceptible individuals with time and used it to make a short-term risk assessment of the COVID-19 epidemic in Hubei Province. Liu et al. (2021) studied the impact of NPIs on COVID-19 transmission by building a fixed-effects regression relationship between NPIs intensity and the time-varying effective reproduction number.

In this study, we formulated a linear spline model to analyze and quantify the time-varying NPIs effectiveness, which can be measured by the proportion of type II cases defined above among all the reported infections. Then, we used the estimated type II case proportion to objectively compute the end-of-outbreak confidence with time at the end of the epidemic.

2. Materials and methods

First, we constructed a mathematical model explicitly accounting for the NPIs effectiveness in the transmission process of COVID-19 in early 2020 in Wuhan. Second, based on the estimated NPIs effectiveness with time, the end-of-outbreak probability was computed since the last reported local infections.

2.1. Data source

In this study, we designed an epidemiological model to describe the COVID-19 outbreak in early 2020 in Wuhan, and we collected the daily number of reported cases as in S1. Table from multiple sources: the case numbers from December 8, 2019, to January 17, 2020, are from two published articles (Li et al., 2020; Pan et al., 2020); the case data from January 18, 2020, to March 24, 2020, are publicly available from the official website of the Health Commission of Hubei Province at http://wjw.hubei.gov.cn/bmdt/dtyw/ (Health Commission of Hubei Province, 2021). It is worth noting that although the diagnosis guidelines experienced adjustments, only if one individual met the diagnosis criteria at the time of being surveyed, would he/she be counted as the infected case in S1. Table, irrespective of whether there are symptoms or not. Moreover, the timeline of the major nonpharmaceutical interventions (NPIs) implemented during this COVID-19 outbreak was summarized in S2. Table.

2.2. Estimate the NPIs effectiveness

We present how a statistical model is constructed to quantify the NPIs effectiveness during the epidemic. In this exercise, the term NPIs effectiveness exclusively refers to the effect of reducing the proportion of the type II cases among all the infections, differing from the namesake measured by the relative reduction in the effective reproduction number (Haug et al., 2020; Bo et al., 2021; Liu et al., 2021), or the relative reduction of the infected cases or deaths (Mendez-Brito et al., 2021). Since the implemented NPIs

aim to cut off the effective contact between the susceptible individuals and the infected individuals, the proportion of the infected cases who are restricted due to NPIs among all the infections can be used to measure the effectiveness of NPIs. Following the dichotomization of type I case and type II case, the greater the proportion of the type II cases, the worse the NPIs effectiveness. Mathematically, the NPIs effectiveness is equal to one minus the proportion of type II cases that possess the chance to cause secondary transmission. For example, if 76% of all the infections are the type II case, the NPIs effectiveness is 24%, *i.e.*, the proportion of the type I cases who are completely restricted by NPIs among all the infections.

As an emerging infectious disease, COVID-19 did not attract public attention at the very beginning of the outbreak in Wuhan. However, once its high transmissibility and deadly pathogenicity were recognized, a series of strict measures were taken to slow the spread of the disease, especially the lockdown of Wuhan City, which was implemented on January 23, 2020, which is denoted as T_1. We regarded the period before T_1 as the free-transmission period of COVID-19 in Wuhan, *i.e.*, all the reported cases I_t had the chance to produce secondary transmission. In contrast, from T_1 on, extensive NPIs policies targeted at cutting off the contact of susceptible individuals with individuals with suspected infection were continuously implemented until the end of the epidemic. The last confirmed case in Wuhan was reported on March 24, 2020, which is denoted as T_2. In this period from T_1 to T_2 (hereinafter referred to as the transmission period under intervention), we assume that all the secondary infections were caused by the infective people not covered by the NPIs restrictions and let the number of these infective cases, *i.e.*, type II cases at day t, be I_t^e. Considering that the daily intensity and efficiency of the NPIs in implementation varied over time, the NPIs effectiveness can be written as a function of time $q_t (0 < q_t < 1)$. Immediately, we assume that the expected number of type II cases I_t^e is the binomial sample from the total reported cases I_t with the sampling probability $1 - q_t$. Throughout the epidemic, the daily number of type II cases I_t^e is summarized as

$$\begin{cases} I_t^e = I_t, & t < T \\ I_t^e \sim B(I_t,\ 1-q_t), & t \geqslant T_1 \end{cases} \tag{1}$$

To obtain the estimation of the NPIs effectiveness q_t as the function of time, we introduce the linear spline (LS) model with different knot numbers ($K = 8, 16, 24, 32, 36$). For the linear spline, we assume u_j is the weight of each linear function and $(t-\kappa_j)_+$ is the j-th linear function with a knot at κ_j, thereby giving the following linear splines:

$$\text{logit}\{q_t\} = \beta_0 + \beta_1 \cdot t + \sum_{j=1}^{K} u_j \cdot (t-\kappa_j)_+ \tag{2}$$

Note that $(t-\kappa_j)_+$ is zero if time t is below the j-th knot κ_j and a positive value otherwise, *i.e.*,

$$(t-\kappa_j)_+ = \begin{cases} t-\kappa_j & \text{if } t-\kappa_j > 0 \\ 0 & \text{if } t-\kappa_j \leq 0 \end{cases}. \tag{3}$$

The linear spline in Eqs. (2) and (3) allows for a wide variety of shapes to be fit with the great versatility. By defining more knots or shifting the existing knots, the linear spline can be easily modified to better fit the data of interest. However, it is also essential to pick the optimal number of knots to avoid under- or over-fitting the data. More details on the linear spline are provided in (Ruppert, 2002; Griggs, 2013).

In this study, we employ the adjusted renewal Equation (Wallinga and Lipsitch, 2007) to describe the transmission dynamics of COVID-19 in Wuhan. Let f_τ be the probability mass function (PMF) of generation time, defined as the interval between the time when one case was infected and the time when the secondary case was infected by him or her. Then, the expected number of all infections at day t caused by the infective type II cases before t, *i.e.*, $I_1^e, \cdots, I_{t-1}^e$, is given by

$$\mu_t = R_0 \left(\sum_{s=1}^{t-1} f_s I_{t-s}^e \right), \tag{4}$$

where R_0 is the basic reproduction number, which is the average number of secondary cases generated by one infectious individual among the susceptible population at the initial time of the epidemic. Therefore, if we assume that the daily number of new infections I_t follows the Poisson distribution with expectation μ_t, the following likelihood function can be designed to obtain the maximum likelihood estimation (MLE) of the unknown parameters $\Theta = \{\beta_0, \beta_1, u_1, \cdots, u_K\}$:

$$L(\Theta; I_t) = \prod_{t=T_1}^{T_2} \frac{e^{-\mu_t} \cdot {\mu_t}^{I_t}}{I_t!}. \tag{5}$$

T_2 here is the day of the last reported case in the epidemic, referring to March 24, 2020, in our case. Since the estimated R_0 of COVID-19 has a wide range from 1.4 to 6.49 (He et al., 2020; Liu et al., 2020; Rahman et al., 2020; Zhao et al., 2020a,b) owing to the diverse sample data and parameter estimation approaches, we set the reproduction number in Eq. (4) with constants of 1.5, 2.0, 3.0, 4.0, 5.0 and 6.0 respectively. For each pre-set value of R_0, five set of estimated values of unknown parameters Θ are obtained by minimizing the negative log-likelihood of $L(\Theta; I_t)$ with five different knot numbers ($K = 8, 16, 24, 32, 36$). And the estimation of Θ corresponding to each R_0 is finalized by selecting knot number with the minimum AICc (the corrected Akaike information criterion) as follows,

$$\text{AICc} = 2k - 2\ln\left(\widehat{L}\right) + \frac{2k^2 + 2k}{n-k-1} \tag{6}$$

where $\widehat{L}$ is the maximum likelihood value of $L(\Theta; I_t)$, k denotes the number of parameters to be estimated, *i.e.*, $K+2$ and n denotes the sample size $T_2 - T_1 + 1$. Thus, the role of varying reproduction numbers in determining the parameter estimation can be explored.

In addition, for each combination of a constant reproduction number and the preset knot number, we resampled the estimated parameters of the NPI effectiveness $\widehat{q}_t$ 1000 times; therefore, the 95% confidence interval (95% CI) of $\widehat{q}_t$ can be summarized based on the bootstrap method.

2.3. Compute the probability of the end of an outbreak

In this section, we aim to compute the probability of giving the end-of-outbreak declaration at the late stage of the COVID-19 outbreak in Wuhan. With each of the 1000 resampled NPIs effectiveness $\widehat{q}_t$, the epidemic curve of infective cases I_t^e is recalculated according to the following equations:

$$\begin{cases} I_t^e = I_t, & t < T_1 \\ I_t^e \sim \text{Binomial}(I_t,\ 1-\hat{q}_t), & t \geqslant T_1. \end{cases} \tag{7}$$

Because the last confirmed case in Wuhan was reported on March 24, 2020, we try to project the trajectory of new cases reappearing after March 25, 2020, by taking the following iterative steps for each estimated parameter set $\widehat{q}_t$:

(i) From March 25, 2020, the expected number of new cases μ_s on day s could be computed by using the adjusted renewal equation based on the binomially sampled unquarantined cases I_t^e $(t < s)$;

(ii) The infective type II cases I_t^e can be sampled binomially with success probability $1 - \widehat{q}_t$ from the reported number of daily cases I_t if t is prior to March 25, 2020 $(t \le T_2)$, or with the success probability $1 - \widehat{q}_{T_2}$ from the expected number of new cases μ_t computed in step (i) if t is after March 24, 2020 $(t > T_2)$. It is worth noting that here, we assume that the NPIs effectiveness after March 25, 2020, is invariant, with the same value as that on March 24, 2020;

(iii) The expected case number μ_{s+1} and the type II case number I_{s+1}^e on the next day $s+1$ can be calculated in the same way, and the iteration was continued until April 30, 2020, which is denoted as T_3. The period from T_2 to T_3 is thus referred to as the end-of-outbreak period.

In Section 2.2, we have obtained $N(=1000)$ estimations of the NPIs effectiveness parameters $\widehat{q}_t$ as the function of time from T_1 to T_2. In the current section, we use each of the estimated $\widehat{q}_t$ to project the trajectory of the daily cases emerging after T_2 following the day-by-day iterations (i)–(iii), then we have 1000 projected trajectories of the expected cases per day from T_2 to T_3. Summarizing the number of expected cases on each day at specific quantiles, *i.e.*, 0.025 quantile, 0.5 quantile and 0.975 quantile, the value range of the expected cases with 95% confidence can be obtained instantly.

For each trajectory X_s, if the predicted daily number of new infections is consistently less than one from some given day s, we set $\delta(X_s) = 1$; otherwise, $\delta(X_s) = 0$. The probability that no additional cases are reported after day s can be defined as

$$P_s = \frac{\sum_{i=1}^{N} \delta(X_{s,i})}{N} \times 100\%, \tag{8}$$

where $i = 1, 2, \cdots N$ represents each trajectory. Therefore, we can declare that the epidemic is over after day s with 95% confidence if $P_s \ge 95\%$.

In summary, the methodological scheme to complete the above computation is shown in Fig. 1. The procedure of parameter estimation is performed in the transmission period under intervention, and we project the probability of epidemic termination in the end-of-outbreak period.

2.4. Summarize assumptions

In summary, along with the above modeling analysis, the following critical assumptions are proposed:

- We only considered the reported cases published within one city but ignored the cases exported to other places or imported from outside;

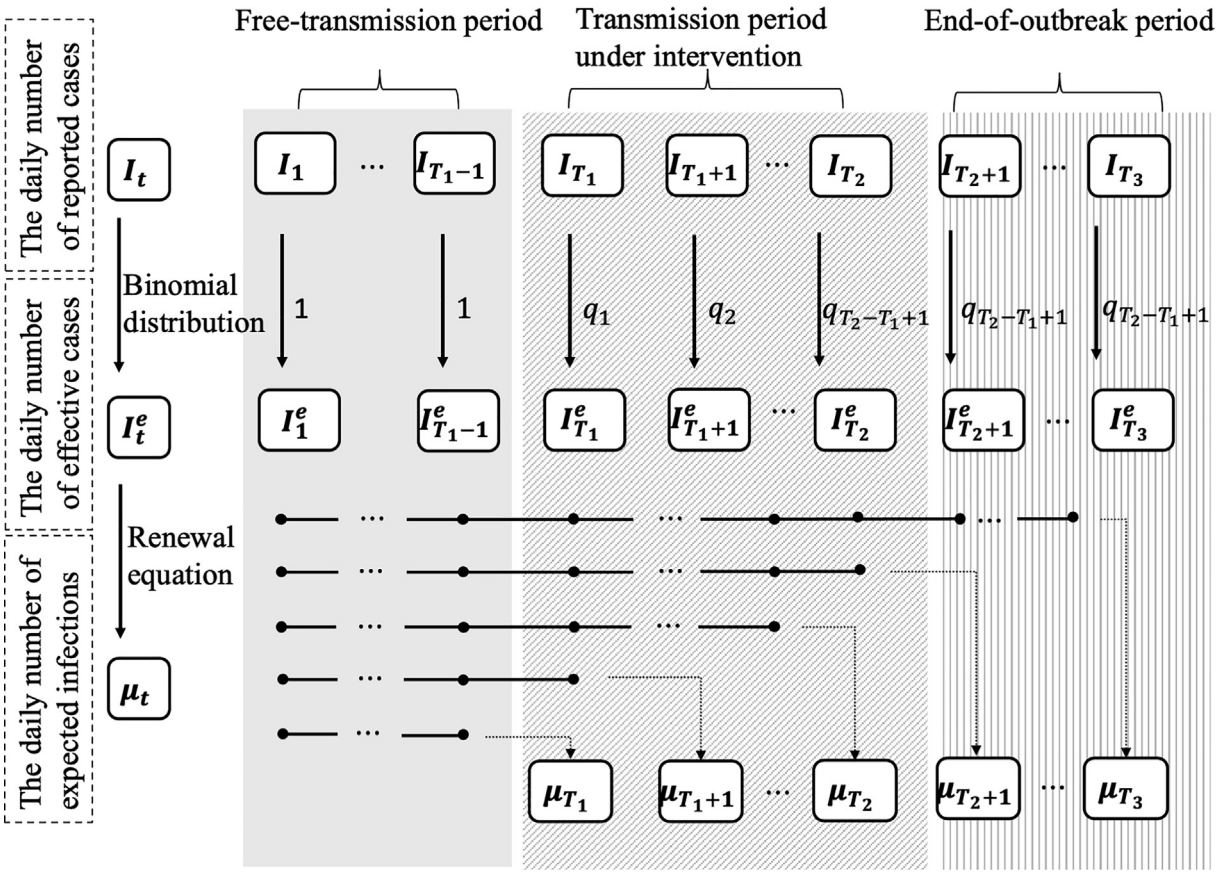

Fig. 1. Scheme plot projecting the end-outbreak probability in the COVID-19 epidemic in Wuhan in early 2020. The entire epidemic period is divided into three periods: the free-transmission period, the transmission period under intervention and the end-of-outbreak period. I_t is used to describe the daily number of the total reported cases at day t; I_t^e represents the daily number of infective cases missing the NPIs restriction, *i.e.*, the type II cases defined in the main text. μ_t represents the daily number of expected infections caused by infective cases prior to day t following the adjusted renewal equation, where the black dots correspond to I_t^e at the same time. q_t denotes the NPIs effectiveness, and $1 - q_t$ is the proportion of infective cases among all the reported cases. In the free transmission period, there are no interventions, so q_t is set as one, while the time-varying q_t $(1 \le t \le T_2 - T_1 + 1)$ are the unknown parameters we need to estimate. In the end-of-outbreak period, q_t is invariably set to be the same as $q_{T_2-T_1+1}$.

- The probability distribution of the generation time was invariant over time with a mean of 5.1 days and a standard deviation of 5.3 days;
- We did not consider the time delay in relation to the reporting time of cases, for example, the time delay from infection to report and the time delay from symptom onset to report.
- During the whole study period, reinfection of the recovered cases was excluded, and all the reported infections were caused by human-to-human transmission.

3. Results

According to the published articles (Li et al., 2020; Pan et al., 2020) and the official report of the Health Commission of Hubei Province (Health Commission of Hubei Province, 2021), the earliest confirmed cases of COVID-19 in Wuhan date back to December 8, 2019. On January 23, once the rapid spread of the infectious disease was recognized, the city was placed under lockdown. With the implementation of various strict control interventions, the outbreak came to an end in late March 2020. The last case was suspected of being infected in the hospital where the individual worked. Even though there was one additional case confirmed in April according to the report of the Health Commission of Hubei Province, he was not included in this study because this case had no direct contact with other susceptible people: the case reported on April 1, 2020, was imported from the UK and acquired a complete quarantine upon arrival at Wuhan. Thus, the epidemic curve of the reported cases per day in Wuhan is shown as the bar plot in Fig. 1. Note that there is an extraordinarily high number of reported cases on February 13, which is the accumulated report of the previous cases due to case correction.

Even though the effective reproduction number R_t is not involved in the modeling framework, for the purpose of exhibiting time-varying transmissibility during the epidemic, R_t and its confidence interval were estimated with the R package EpiEstim developed by Cori et al. (2013) as shown in Fig. 2. The estimation of R_t prior to January 23, 2020 (T_1) fluctuates around a mean size of $\sim$3 and produces a relatively wide confidence interval caused by the sparse number of reported cases at this stage. After T_1, R_t increased rapidly to the highest value of 4 on January 28, 2020, and then showed a wavelike decrease but remained above one until 3 weeks later, which accounted for the largest wave of case growth. On around February 13, we can see a steep ascent from an ongoing downward trend and then a subsequent slow descent, which was definitely caused by the spike number of reported cases on February 13. With the implementation of various interventions, R_t continued to fall below one after February 20, 2020, and the daily number of reported cases was reduced to less than 600 per day, indicating the gradual control over the epidemic. The end of the outbreak was finally declared and the lockdown was lifted on April 8, 2020. A total of 50,008 infections and 2574 deaths were caused in Wuhan City.

For each preset constant basic reproduction number 1.5, 2.0, 3.0, 4.0, 5.0 and 6.0, we obtained the parameter estimation for the linear spline (LS) with different knot numbers 8, 16, 24, 32 and 36, which were used to describe the NPIs effectiveness as a function of time and are shown in Fig. 2. The AIC (Akaike information criterion) and AICc (corrected Akaike information criterion)

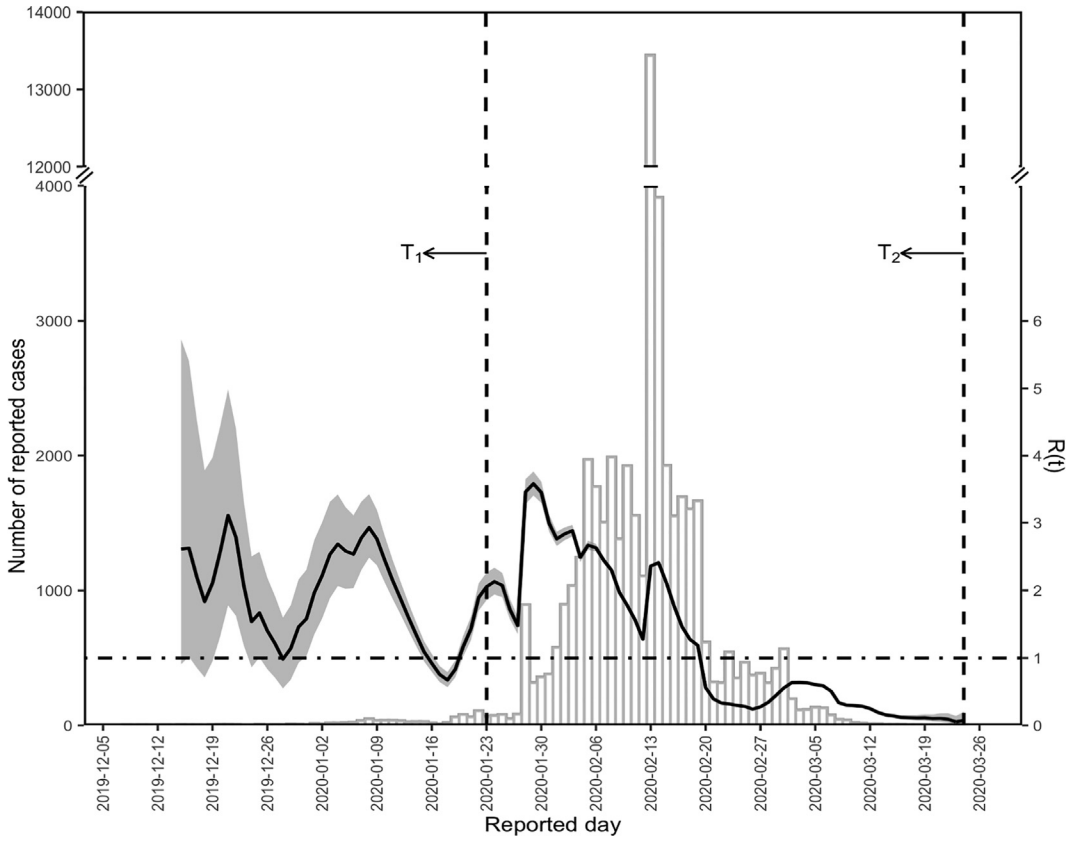

Fig. 2. The epidemic curve of daily reported cases of COVID-19 and the corresponding effective reproduction number. The bar in the figure gives the epidemic curve of the original data of reported cases by day during the COVID-19 epidemic in Wuhan in early 2020. The black solid line is the effective reproduction number R_t over time t, the size of which is measured by the right y-axis. When R_t is above the threshold value one represented by the horizontal dot-dash line, the epidemic is in an increasing trend; otherwise, it is in decline. The left vertical dashed line with an arrow pointing to T_1 (January 23, 2020) is the day when the lockdown started in Wuhan, while the right vertical dashed line with an arrow pointing to T_2 (March 24, 2020) is the day when the last confirmed case was reported.

measuring the goodness of fit for the 60 maximum likelihood estimations are summarized in S3. Table. Under the case of all six preset reproduction numbers, we found that a further increase in the number of knots K is unlikely to decrease the AICc because the AICc at $K = 24$ is smaller than 0.4% times the AICc at $K = 16$. Therefore, all further computations throughout the study are based on the parameter estimations by setting the number of linear spline knots to 24 following the selection criterion of knot number by Ruppert (2002).

For the proportion of infective type II cases that were assumed to cause all the reported infections in our study, the model with different R_0 values produces comparative estimations, as shown in Fig. 3. The degressive maximum estimation of the proportion of type II cases was obtained with the reproduction numbers increasing from 1.5 to 6.0. For the R_0 values of 1.5, 2.0 and 3.0, maximum values of 0.65, 0.60 and 0.53 are observed on 05 February 2020, 03 February 2020, and 30 January 2020, respectively, while for the R_0 values of 4.0, 5.0 and 6.0, the maximum estimation of 0.5 is on the first day of intervention implementation, *i.e.*, T_1. For the three greater R_0 values of 4.0, 5.0 and 6.0, the continuous decline in estimation indicates that the strict NPIs measures succeeded in permitting fewer cases to produce secondary transmission throughout the population with time, and the declining trend agrees with the decreasing transmissibility reflected by the effective reproduction number. However, the estimation based on the smaller R_0 values of 1.5, 2.0 and 3.0 descended more slowly after the day with the maximum estimation. For all six reproduction numbers, the proportions of type II cases decayed to the near-zero level until the end of the transmission period under intervention. This discrepancy suggests that the decreasing pattern is to some extent influenced by the different assumptions about the reproduction numbers and essentially reflects the balance between infectious disease transmissibility and intervention intensity when fitting the reported epidemic curve.

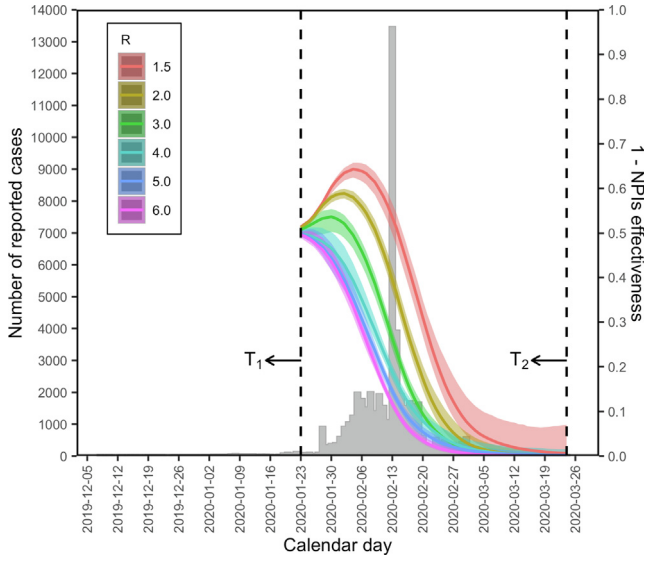

Fig. 3. Comparison of the NPIs effectiveness estimated by the linear spline (LS) with varying reproduction numbers. The epidemic curve of daily reported cases is given in the bar graph. The solid line and its corresponding ribbon in the same color are the median and 95% confidence interval of the estimated NPIs effectiveness for each preset reproduction number, 1.5, 2.0, 3.0, 4.0, 5.0 and 6.0. The linear spline model is constructed with 24 knots. The left vertical dashed line with an arrow pointing to T_1 (January 23, 2020) is the day when the lockdown started in Wuhan. The right vertical dashed line with an arrow pointing to T_2 (March 24, 2020) is the day when the last confirmed case was reported. The size of the estimated NPIs effectiveness is measured by the right y-axis.

In Fig. 4, we show the projected number of expected cases over time from March 24, 2020, when the last confirmed cases were reported, until April 30, 2020. The median numbers of new cases per day computed by all six reproduction numbers present a continued declining trend, and the 95% confidence intervals shrink over time. In addition, the earliest dates when the predicted case number goes below one, *i.e.*, the end-of-outbreak day with 95% confidence were reached 05 April, 02 April, 02 April, 04 April, 03 April, and 01 April, corresponding to R_0 values of 1.5, 2.0, 3.0, 4.0, 5.0 and 6.0, respectively. Here, we set the daily case number calculated from mathematical models smaller than the integer one to be zero case, *i.e.*, indicating no infection on this day. Furthermore, Fig. 5 explicitly illustrates the probability of end-of-outbreak declaration over time during the late period of the epidemic, and the first days when the probability is greater than 95% agree with that in Fig. 4 just listed above. For the six preset R_0 values, the end-of-outbreak probability experienced a quick increment over time during the beginning of April from the near-zero level to the higher near-one level and persisted until the end of the research period. It should be noted that the lockdown in Wuhan was lifted on April 8, 2020. When we look into the daily number at the late stage of the outbreak, the last case was reported unexpectedly on March 24. But the estimated proportion of type II case on this day is extremely small (See Fig. 3), which means the possibility of the last reported case to cause further transmission is tiny and the influence of the only last reported case on the predicted elimination date is also insignificant in our modeling framework. Since there have been five continuous days without new cases before March 24, it is possible that the ending probability of the outbreak increases rapidly to a high level after the low-risk days. In the end, we conducted the sensitivity analysis of varying the threshold defining no daily infection from one to smaller values of 0.7, 0.5, 0.3 and 0.1 towards the final projection of the end-of-outbreak days in Fig. 6. Overall, varying thresholds produce the undifferentiated trend of the ending probability of the outbreak over time. While the greater threshold corresponds to the earlier end-of-outbreak days with 95% confidence, setting a smaller threshold will

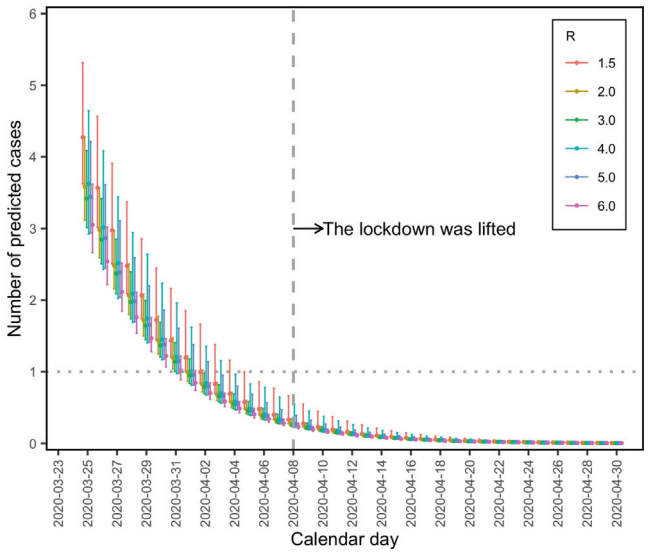

Fig. 4. Comparison of the predicted case numbers by the linear spline (LS) with varying reproduction numbers. The dots and error bars in the same color are the median number of predicted cases calculated under the LS method, with 24 knots for each preset reproduction number of 1.5, 2.0, 3.0, 4.0, 5.0 and 6.0. The extended whisker represents the 95% confidence interval. The vertical dashed line is the day when the actual lockdown was lifted. The horizontal dotted line at case number one gives the reference for epidemic termination.

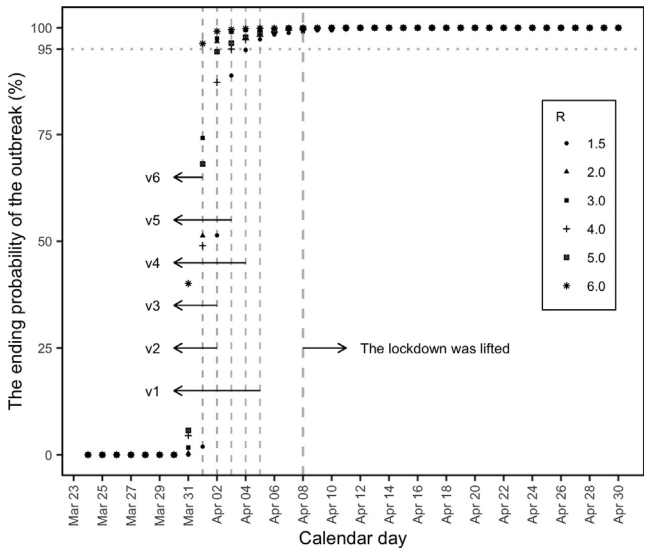

Fig. 5. Comparison of the projected end-of-outbreak probability by the linear spline (LS) with varying reproduction numbers. The projected probability of the end of the outbreak over time after the last reported case is shown with different shapes of points for the LS method with 24 knots. The five gray vertical dashed lines v1, v2, v3, v4, v5 and v6 represent the earliest day when the probability reaches 95% for each preset reproduction number of 1.5, 2.0, 3.0, 4.0, 5.0 and 6.0. The rightmost gray dashed line is the day when the lockdown was actually lifted, namely, April 08, 2020. The horizontal dotted line gives the reference for the 95% probability.

ensure the inherent risk of infection at a lower level and thus postponed the end-of-outbreak day.

4. Discussion

In this study, we performed a retrospective epidemiological assessment of the time-varying effectiveness of the NPIs policy implemented in the 2019–2020 epidemic of COVID-19 in Wuhan by developing a new model to explicitly parameterize the NPIs effectiveness as a function of time. The model was constructed directly based on the daily number of reported cases in Wuhan without distinguishing symptoms and is therefore applicable to other epidemic curves, such as the epidemic curve based on illness onset. In the model, we did not clearly distinguish the intervention items implemented during this epidemic but exclusively attributed the change in epidemic growth to the effect of NPIs cutting off the contact of infected cases with the susceptible population. Even though (Lee, 2019) has proposed the distinct transmission modes may cause the resurgence of the Ebola virus disease (EVD), we did not make the similar distinction of the COVID-19 transmission mode in the current study, but separated the reported cases according to whether the case received NPIs restrictions prior to developing infectiousness or not. Therefore, the reported cases were classified into two types: i) cases that could no longer cause secondary infection due to timely and effective quarantine or isolation constraints and ii) infective cases that were a potential source of further transmission due to imperfect or missing NPIs. The estimated results showed that the increasing patterns of NPIs

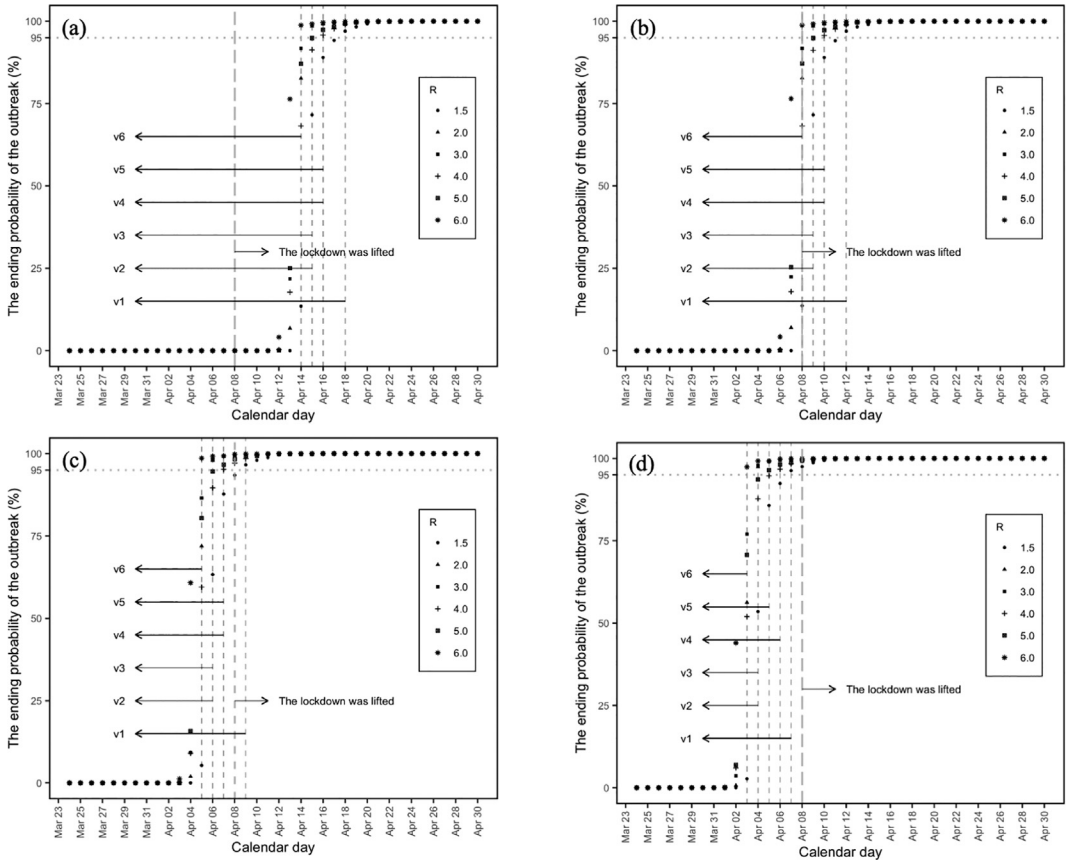

Fig. 6. Comparison of the projected end-of-outbreak probability by the linear spline model with varying thresholds defining no daily infection. From (a) to (d), the thresholds to define no daily infection are 0.1, 0.3, 0.5 and 0.7 respectively.

effectiveness with time differ slightly from the reproduction numbers, indicating the balanced interaction between transmissibility and intervention intensity during the epidemic.

On the other hand, based on the estimated NPIs effectiveness parameter, we proposed an iterative method to project the expected case number from the reported day of the last confirmed case to the end of April, and thus, the end-of-outbreak probability per day during this period was computed. In our results, the projected end-of-outbreak probability was surprisingly sensitive to the calendar day at the beginning of April, featuring a leaping increment with each day. This sensitivity highlights the necessity of using great caution when declaring the termination of the outbreak. The varying preset reproduction number in our project results in different timings of the end-of-outbreak declaration with 95% confidence. Intuitively, the greater transmissibility of the pathogen, the harder to control the outbreak and thus the later date of elimination to be expected for higher R_0. However, this intuition is not always exact. Essentially, the elimination of the outbreak is the result of the balanced interaction between transmissibility of the pathogen and intervention intensity during the epidemic. In our modeling framework, the NPIs effectiveness parameter $\widehat{q}_t$ which was closely related to the proportion of type II cases was estimated to best fit the reported epidemic curve. When the reproduction number R_0, *i.e.*, the metrics of epidemic transmissibility is larger, the NPIs effectiveness should be estimated greater compared with that of the less infectious epidemics to bring the outbreak under control. With the more intensive implementation of NPIs, it is possible to expect an earlier date of elimination as larger R_0. However, it is also noteworthy that if the pre-set R_0 is too greater than the actual value, the overestimation of the NPIs effectiveness is possible, resulting in advanced projection of the epidemic elimination. Moreover, all the days of the end-of-outbreak declaration projected using the six preset reproduction numbers were earlier than the day when the lockdown was lifted. This discrepancy reflects the difference in judgment criteria based on stiff epidemiological surveillance practice and flexible mathematical simulation modeling transmission dynamics. Undoubtedly, a later declaration of epidemic termination is well advised when focusing on the high risk of epidemic recurrence, but we must acknowledge that intense interventions are very likely to bring about the end of the outbreak at an earlier date, which is also a key point our model highlights.

There are two lessons to be learned from our exercise. First, we classified reported cases into two types based on whether the case was effectively treated. This distinguishment explicitly highlights the fact that not every case had the chance to cause the secondary transmission in the context of NPIs' implementation and only the cases missing NPIs restrictions contributed to continuing the transmission of the pathogen. Comparing with making no such distinction where the end-of-outbreak confidence was projected on the basis of all the infected cases (Nishiura et al., 2016), the distinction here would be likely to advance the projected date of epidemic elimination, as shown in Fig. 7. That is because the dichotomization of infected cases has exclusively attributed the epidemic elimination to the infective cases unrestricted by NPIs, rather than all the infected cases. Second, the declaration of the end of the epidemic was conventionally based on two incubation periods, but other infectious disease outbreaks, such as MERS (Nishiura et al., 2016) and Ebola (Lee and Nishiura, 2019), have shown that this way to define the termination of an outbreak is not always correct. A customized scheme to correctively predict epidemic termination should be made to take full account of the specific outbreak context like the implementation of NPIs. Even though declaring the termination of the epidemic at a later date is more reliable, it would be beneficial to the mental health of the individual and the social order to return to normal as early as possible by lifting

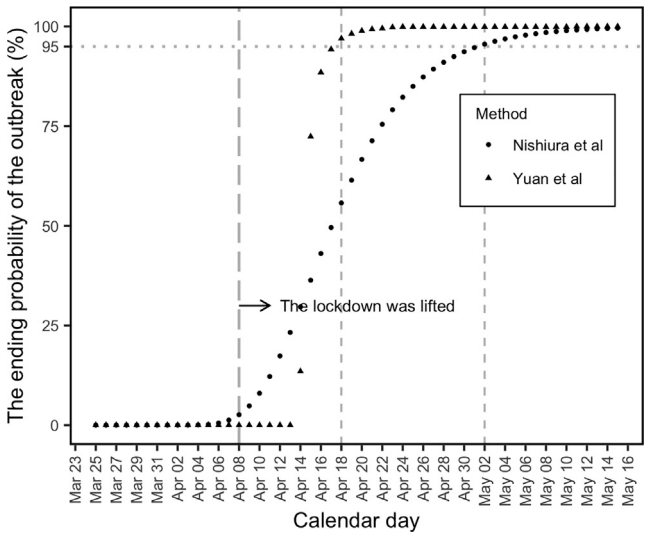

Fig. 7. Comparison of the projected end-of-outbreak probability by the linear spline model with that by the method of Nishiura et al. (2016). For both models, the same generation time distribution was used as in the main text. The other tunable parameters used in the linear spline model included: the basic reproduction number $R_0 = 1.5$, the number of knots being 24 and the threshold to define no daily infections being 0.1, and Nishiura et al. (2016) included the dispersion parameter being 0.7 which governing the variation of the individual infectiousness.

the ban of quarantine and lockdown according to the theoretically predicted end-of-outbreak day. Policy-makers must be radical enough to balance the public demand for earlier removal of restrictions and the anti-epidemic reliability of prolonged NPIs.

The present study was not free from limitations. First, we have to acknowledge that with the increasing understanding about the COVID-19 and the improved epidemiological surveillance since its emergence, the reporting process involving the issues of reporting delay and underreporting would not be changeless throughout the whole epidemic period. The current study rested on reported cases without considering the reporting delay from infection, from illness onset or from confirmation of infection. If involving the time delay, the practical declaration of the end of the outbreak should have been given several days earlier than our prediction. On the other hand, the underreporting issue, *i.e.*, some cases not being reported, would result in undercounting the absolute number of the infected cases and hence postponing the predicated date of the epidemic elimination depending on the size of underreporting rate. Also note that if the underreporting rate is time-invariant throughout the epidemic, it seems not to influence the estimation of NPIs effectiveness since the following two events are epidemiologically independent, *i.e.*, i) case to be reported or not and ii) case belonging to type II or not. Quantifying the effect of the time-varying reporting process on the projection of the end-of-outbreak confidence is beyond the scope of this study and would be the next topic to improve our modeling scalability. Second, we assumed invariant distribution parameters of the generation time over time, but Hart et al. (2022) concluded that the mean generation time would shorten greatly as the epidemic continued. Thus, the time-varying NPIs effectiveness under our assumption must have been underestimated, especially in the late period of the epidemic, and the predicted end-of-outbreak day was also delayed. The influence of varying generation time during the different epidemic periods on the end-of-outbreak prediction is our next research focus. Third, this epidemic transmission was complicated by multiple infection modes, including common source infections and propagated infections. In our models, all the reported cases were dichotomized depending on whether one case received effective intervention, and we assumed that the secondary infections

were exclusively produced by the infective cases, ignoring the common source infections. Fourth, to accommodate the change in diagnostic criteria and case definition at the beginning of the epidemic, the original case data we used in this study were corrected by the local government two times, on February 13 and February 21, 2020. The misreported or unreported cases in the past were accumulatively reported on the two days, but we fit them directly instead of redistributing these cases in our model because we believe this correction occurred at the very beginning of the epidemic, posing little effect on the parameter estimation and end-of-outbreak prediction in the later stage of the epidemic, and the model we proposed features the direct use of the reported cases as well. Fifth, the current model did not include the variation in individual infectiousness which was closely linked to the superspreading events (Chen et al., 2021), though six pre-set reproduction numbers were independently simulated to project the end-of-outbreak probability. The impact of overdispersed transmission of SARS-CoV-2 on the probability projection needs to be considered further.

In summary, we have proposed an objective model to dichotomize all the reported cases into two types based on whether the cases received effective intervention before evolving infectiousness. By estimating the time-varying NPIs effectiveness under six different reproduction numbers, the timings of the end-of-outbreak declaration were projected, and we acknowledged that the timings were very sensitive to the size of the basic reproduction number. The timing discrepancy of the end-of-outbreak declaration caused by epidemiological surveillance criteria and mathematical modeling criteria highlights the potential for intense interventions to bring about the end of the outbreak within one incubation period after the last confirmed case. How to predict the exact end-of-outbreak time by including the varying generation time distributions over time remains an open question, toward which we may combine the mathematic model with the data-driven approaches (Liu et al., 2021) in our next study.

5. Ethics approval and consent to participate

In the present study, we analyzed data that are publicly available. As such, the data sets used in this study were de-identified and fully anonymized; the analysis of publicly available data with no identifying information does not require ethical approval.

Funding

This work was supported by the National Natural Science Foundation of China (Grant Nos. 62172164, 12026608 and 12031010), Guangdong Basic and Applied Basic Research Foundation (Grant Nos. 2019B151502062 and 2021A1515012317). The funders had no role in the study design, data collection and analysis, decision to publish, or preparation of the manuscript.

CRediT authorship contribution statement

Baoyin Yuan: Conceptualization, Methodology, Data curation, Software, Visualization, Writing – original draft. **Rui Liu:** Supervision, Writing – review & editing, Funding acquisition. **Sanyi Tang:** Validation, Supervision, Writing – review & editing.

Declaration of Competing Interest

The authors declare that they have no known competing financial interests or personal relationships that could have appeared to influence the work reported in this paper.

Acknowledgment

This work was supported by the National Natural Science Foundation of China (Grant Nos. 62172164, 12026608 and 12031010), Guangdong Basic and Applied Basic Research Foundation (Grant Nos. 2019B151502062 and 2021A1515012317). The funders had no role in the study design, data collection and analysis, decision to publish, or preparation of the manuscript.

Appendix A. Supplementary data

Supplementary data to this article can be found online at https://doi.org/10.1016/j.jtbi.2022.111149.

References

Akhmetzhanov, A.R., Jung, S., Cheng, H.Y., Thompson, R.N., 2021. A hospital-related outbreak of SARS-CoV-2 associated with variant Epsilon (B.1.429) in Taiwan: transmission potential and outbreak containment under intensified contact tracing, January–February 2021. Int. J. Infect. Dis. 110, 15–20. https://doi.org/10.1016/j.ijid.2021.06.028.

Atkeson, A., Droste, M.C., Mina, M., Stock, J.H., 2020. Economic benefits of COVID-19 screening tests. medRxiv 10.22.20217984. https://doi.org/10.1101/2020.10.22.20217984.

Bo, Y., Guo, C., Lin, C., Zeng, Y., Li, H.B., Zhang, Y., et al., 2021. Effectiveness of non-pharmaceutical interventions on COVID-19 transmission in 190 countries from 23 January to 13 April 2020. Int. J. Infect. Dis. 102, 247–253.

Centers for Disease Control and Prevention, CDC, 2021. Science brief: options to reduce quarantine for contacts of persons with SARS-CoV-2 infection using symptom monitoring and diagnostic testing. COVID-19. https://www.cdc.gov/coronavirus/2019-ncov/science/science-briefs/scientific-brief-options-to-reduce-quarantine.html#print. Accessed 24 November 2021.

Chen, P., Koopmans, M., Fisman, D., 2021. Understanding why superspreading drives the COVID-19 pandemic but not the H1N1 pandemic. Lancet Infect. Dis. 21 (9), 1203–1204.

Cori, A., Ferguson, N.M., Fraser, C., Cauchemez, S., 2013. A new framework and software to estimate time-varying reproduction numbers during epidemics. Am. J. Epidemiol. 178 (9), 1505–1512. https://doi.org/10.1093/aje/kwt133.

Djaafara, B.A., Imai, N., Hamblion, E., Impouma, B., Donnelly, C.A., Cori, A., 2021. A quantitative framework for defining the end of an infectious disease outbreak: application to Ebola virus disease. Am. J. Epidemiol. 190 (4), 642–651. https://doi.org/10.1093/aje/kwaa212.

Du, Z., Pandey, A., Bai, Y., Fitzpatrick, M.C., Chinazzi, M., Piontti, A.P., et al., 2021. Comparative cost-effectiveness of SARS-CoV-2 testing strategies in the USA: a modelling study. Lancet Public Health 6 (3), e184–e191.

Elliott, L., 2020. The past three months have proved it: the costs of lockdown are too high Accessed 20 October 2021 Economics Viewpoint https://www.theguardian.com/business/2020/jun/14/the-past-three-months-have-proved-it-the-costs-of-lockdown-are-too-high.

Griggs, W., 2013. Penalized spline regression and its applications Available at:. Whitman College.

Guangzhou Municipal Health Commission, 2021. The latest report of COVID-19. http://wjw.gz.gov.cn/ztzl/xxfyyqfk/yqtb/content/post_7337795.html. Accessed 25 October 2021.

Hart, W.S., Abbott, S., Endo, A., Hellewell, J., Miller, E., Andrews, N., et al., 2022. Inference of the SARS-CoV-2 generation time using UK household data. eLife 11. https://doi.org/10.7554/eLife.70767.

Haug, N., Geyrhofer, L., Londei, A., Dervic, E., Desvars-Larrive, A., Loreto, V., 2020. Ranking the effectiveness of worldwide COVID-19 government interventions. Nat. Hum. Behav. 4 (12), 1303–1312.

He, D., Zhao, S., Xu, X., Lin, Q., Zhuang, Z., Cao, P., et al., 2020. Low dispersion in the infectiousness of COVID-19 cases implies difficulty in control. BMC Public Health. 20, 1558. https://doi.org/10.1186/s12889-020-09624-2.

Health Commission of Hubei Province, 2021. Epidemic situation of COVID-19 in Hubei Province. http://wjw.hubei.gov.cn/bmdt/dtyw/. Accessed 25 October 2021.

Kucharski, A., Klepac, P., Conlan, A.J.K., Kissler, S.M., Tang, M.L., Fry, M.M.H., et al., 2020. Effectiveness of isolation, testing, contact tracing, and physical distancing on reducing transmission of SARS-CoV-2 in different settings: a mathematical modelling study. Lancet Infect. Dis. 20 (10), 1151–1160.

Lee, H., Nishiura, H., 2019. Sexual transmission and the probability of an end of the Ebola virus disease epidemic. J. Theor. Biol. 471, 1–12. https://doi.org/10.1016/j.jtbi.2019.03.022.

Li, Q., Guan, X., Wu, P., Wang, X., Zhou, L., Tong, Y., et al., 2020. Early transmission dynamics in Wuhan, China, of Novel Coronavirus-Infected Pneumonia. N. Engl. J. Med. 382 (13), 1199–1207.

Liang, S.T., Liang, L.T., Rosen, J.M., 2021. COVID-19: a comparison to the 1918 influenza and how we can defeat it. Postgrad. Med. J. 97 (1147), 273–274. https://doi.org/10.1136/postgradmedj-2020-139070.

Linton, N.M., Akhmetzhanov, A.R., Nishiura, H., 2021. Localized end-of-outbreak determination for coronavirus disease 2019 (COVID-19): examples from

clusters in Japan. Int. J. Infect. Dis. 105, 286–292. https://doi.org/10.1016/j.ijid.2021.02.106.
Liu, Y., Gayle, A.A., Wilder-Smith, A., Rocklöv, J., 2020. The reproductive number of COVID-19 is higher compared to SARS coronavirus. J. Travel Med. 27 (2), 1–4. https://doi.org/10.1093/jtm/taaa021.
Liu, Y., Morgenstern, C., Kelly, J., Lowe, R., Jit, M., 2021a. The impact of non-pharmaceutical interventions on SARS-CoV-2 transmission across 130 countries and territories. BMC Med. 19 (1). https://doi.org/10.1186/s12916-020-01872-8.
Liu, R., Zhong, J., Hong, R., Chen, E., Aihara, K., Chen, P., Chen, L., 2021b. Predicting local COVID-19 outbreaks and infectious disease epidemics based on landscape network entropy. Sci. Bull. 66 (22), 2265–2270.
Mendez-Brito, A., Bcheraoui, C.E., Pozo-Martin, F., 2021. Systematic review of empirical studies comparing the effectiveness of non-pharmaceutical interventions against COVID-19. J. Infect. 83 (2021), 281–293. https://doi.org/10.1016/j.jinf.2021.06.018.
Nanjing Municipal Health Commission, 2021. The latest report of COVID-19 in Jiangsu Province by August 10. http://wjw.nanjing.gov.cn/njswshjhsywyh/202108/t20210811_3099635.html. Accessed 25 October 2021.
Nishiura, H., Miyamatsu, Y., Mizumoto, K., 2016. Objective determination of end of MERS outbreak, South Korea. Emerg. Infect. Dis. 22 (1), 146–148. https://doi.org/10.3201/eid2201.151383.
Nishiura, H., 2016. Methods to determine the end of an infectious disease epidemic: a short review. In: Chowell G, Hyman J, editors. Mathematical and Statistical Modeling for Emerging and Re-Emerging Infectious Diseases. Springer: Cham, pp. 291-301. https://doi.org/10.1007/978-3-319-40413-4_17.
Normile, D., 2021. 'Zero COVID' countries seek exit strategies. Science 373 (6561), 1294–1295. https://doi.org/10.1126/science.acx9099.
Pan, A.n., Liu, L.i., Wang, C., Guo, H., Hao, X., Wang, Q.i., Huang, J., He, N.a., Yu, H., Lin, X., Wei, S., Wu, T., 2020. Association of public health interventions with the epidemiology of the COVID-19 outbreak in Wuhan, China. JAMA 323 (19), 1915.
Parag, K.V., Cowling, B.J., Donnelly, C.A., 2021. Deciphering early-warning signals of SARS-CoV-2 elimination and resurgence from limited data at multiple scales. J. R. Soc. Interface 18, 20210569. https://doi.org/10.1098/rsif.2021.0569.
Parag, K.V., Donnelly, C.A., Jha, R., Thompson, R.N., 2020. An exact method for quantifying the reliability of end-of-epidemic declarations in real time e1008478 PLoS Comput. Biol. 16 (11). https://doi.org/10.1371/journal.pcbi.1008478.
Rahman, B., Sadraddin, E., Porreca, A., 2020. The basic reproduction number of SARS-CoV-2 in Wuhan is about to die out, how about the rest of the World? Rev. Med. Virol. 2020,. https://doi.org/10.1002/rmv.2111 e2111.
Rubin, R., 2021. COVID-19 vaccines vs variants-determining how much immunity is enough. JAMA 325 (13), 1241–1243. https://doi.org/10.1001/jama.2021.3370.
Ruppert, D., 2002. Selecting the number of knots for penalized splines. J. Comput. Graph. Stat. 11 (4), 735–757. https://doi.org/10.1198/106186002853.
Tang, B., Xia, F., Tang, S., Bragazzi, N.L., Li, Q., Sun, X., Liang, J., Xiao, Y., Wu, J., 2020. The effectiveness of quarantine and isolation determine the trend of the COVID-19 epidemic in the final phase of the current outbreak in China. Int. J. Infect. Dis. 96, 636–647.
The British Academy, 2021. The COVID decade: understanding the long-term societal impacts of COVID-19. The British Academy, London.
The Health Commission of Hainan Province, 2021. http://wst.hainan.gov.cn/swjw/rdzt/yqfk/202108/t20210803_3028826.html. Accessed 25 October 2021.
Thompson, R.N., Morgan, O.W., Jalava, K., 2019. Rigorous surveillance is necessary for high confidence in end-of-outbreak declarations for Ebola and other infectious diseases. Phil. Trans. R. Soc. B 374, 20180431. https://doi.org/10.1098/rstb.2018.0431.
UK Health Security Agency, 2020. COVID-19: epidemiological definitions of outbreaks and clusters. https://www.gov.uk/government/publications/covid-19-epidemiological-definitions-of-outbreaks-and-clusters/covid-19-epidemiological-definitions-of-outbreaks-and-clusters-in-particular-settings. Accessed February 5, 2022.
Wallinga, J., Lipsitch, M., 2007. How generation intervals shape the relationship between growth rates and reproductive numbers. Proc. R. Soc. B. 274 (1609), 599–604. https://doi.org/10.1098/rspb.2006.3754.
World Health Organization, WHO, 2017. The yellow fever outbreak in Angola and Democratic Republic of the Congo ends. https://reliefweb.int/report/democratic-republic-congo/yellow-fever-outbreak-angola-and-democratic-republic-congo-ends. Accessed February 5, 2022.
World Health Organization, WHO, 2018. South Sudan declares the end of its longest cholera outbreak. https://www.afro.who.int/news/south-sudan-declares-end-its-longest-cholera-outbreak. Accessed February 5, 2022.
Zhao, S., Lin, Q., Ran, J., Musa, S.S., Yang, G., Wang, W., Lou, Y., Gao, D., Yang, L., He, D., Wang, M.H., 2020a. Preliminary estimation of the basic reproduction number of novel coronavirus (2019-nCoV) in China, from 2019 to 2020: A data-driven analysis in the early phase of the outbreak. Int. J. Infect. Dis. 92, 214–217.
Zhao, S., Lin, Q., Ran, J., Musa, S.S., Yang, G., Wang, W., Lou, Y., Gao, D., Yang, L., He, D., Wang, M.H., 2020b. to 2020: A reply to Dhungana. Int. J. Infect. Dis. 94, 148–150.